Biointerface Research in Applied Chemistry
Platinum Open Access Journal (ISSN: 2069-5837)

Article
Volume 12, Issue 1, 2022, 718 - 731
https://doi.org/10.33263/BRIAC121.718731

Influence of Thickness on the Structural, Morphological and Optical Properties of Co-doped TiO_2 Thin Films Prepared by Sol-Gel Method

Niloofar Mozaffari [1,*], Viola Vambol [2], Yanuar Hamzah [3], Alaa El Din Mahmoud [4], Nastaran Mozaffari [5], Nadeem A khan [6], Sergij Vambol [7], Nishat Khan [8], Arun Vinod [9]

1 Department of Physics, Faculty of Sciences, Science and Research Branch, Islamic Azad University, Tehran, Iran, 1477893855; niloofar.mozaffari1991@gmail.com (N.M.);
2 Department of Applied Ecology and Environmental Sciences, National University "Yuri Kondratyuk Poltava Polytechnic", Poltava, Ukraine; violavambol@gmail.com (V.V.);
3 Department of Physics, Faculty of Mathematics and Natural Sciences, Universitas Riau, Pekanbaru, Indonesia, 28293; yanuar.hamzah@lecturer.unri.ac.id (Y.H.);
4 Environmental Sciences Department, Faculty of Science, Alexandria University, 21511 Alexandria, Egypt; alaa-mahmoud@alexu.edu.eg (A.E.D.M.);
5 Department of Environmental Engineering, Faculty of Natural Resources and Environment, Science and Research Branch, Islamic Azad University, Tehran, Iran, 1477893855; mozaffarinastaran7@gmail.com (N.M.);
6 Department Civil Engineering, Jamia Millia Islamia, New Delhi, India, 110025; er.nadimcivil@gmail.com (N.A. K.);
7 Kharkiv Petro Vasylenko National Technical University of Agriculture, Kharkiv, Ukraine, 61002; sergvambol@gmail.com (S.V.);
8 Environmental Research Lab, Department of Chemistry, AMU, Aligarh, India, 202001; nishatk57@gmail.com (N.K.);
9 Department of Physics, Mar Thoma College, Tiruvalla, Kerala, India, 689103; aruvinod@gmail.com (A.V.);
* Correspondence: niloofar.mozaffari1991@gmail.com (N.M.);

Scopus Author ID 57204328656

Received: 10.03.2021; Revised: 10.04.2021; Accepted: 15.04.2021; Published: 26.04.2021

Abstract: TiO_2-based materials have high strength and suitable electronic properties that make TiO_2 widely used. In this research, Co-doped TiO_2 thin films were created through the sol-gel spin-coating method. The deposition process was conducted 3 times to prepare 1 to 3 layers. The structural, morphological, and optical properties of Co-TiO_2 thin films were explored by XRD, SEM, and UV-VIS analyses. The prepared films were amorphous without a crystalline structure. SEM images demonstrate highly uniform particles on the surfaces. With the rise of thickness, nanoparticles get closer, and the particle size decreases. EDS spectra verify the existence of Ti, O, and Co in all samples. The transparency of thin films was reduced by increasing the thickness. Bandgap energy decreased with increasing the deposition layers, while Urbach energy increased.

Keywords: Co-doped TiO_2 thin films; spin-coating method; sol-gel synthesis; optical properties.

1. Introduction

The suitable electronic properties, less amount of toxicity, and high strength have made Titania (TiO_2) and Titania-based materials popular for various applications in photocatalytic activity [1], solar cells [2], and optical devices [1,3]. Titanium nanoparticles have some other compelling properties, such as chemical durability [3], high amount of dielectric constant and refractive index, and transparency in the visible and near-infrared area [3,4].

However, titanium nanoparticles have some drawbacks. TiO_2 has a wide bandgap that gives rise to a low absorption activity [5-8]. Besides, one major limitation of using TiO_2 as a photocatalyst application is its low photo quantum efficiency and the swift recombination of photogenerated electron-hole pairs [9]. It is reported that using titania alone demonstrates no activity or low activity for photocatalysis [10,11]. In this case, TiO_2 doped with metals possess optimized properties for different applications [12].

Cobalt ion has intriguing properties among various metals, including wide bandgap, interesting ferromagnetic characteristics, and high Curie temperature [13-15]. Herein, we focus on Co^{2+} ions as doping transition metal with TiO_2 because Co^{2+} possesses analogous radius like Ti^{4+} and can easily enter into interstitial lattice sites to modify the nanostructure, create electron-trap in the crystal lattice, decrease the bandgap [16], and broaden some functions like photocatalytic activity [9,17].

Liu *et al.* (2018) [16] have reported that cobalt ion incorporates into TiO_2 crystal structures. Thus, the bandgap is decreased because of the formation of the electron-trap center in the crystal lattice. Regarding some published articles [18-21], metal or non-metal dopants increases capacitive properties of TiO_2 and its absorption shifts to the larger wavelengths. In terms of pollutants removal from water, it was shown in previous studies that titania modified by metals and dopant ions including Ag, Pd, Ru, Pt, Cu and Fe^{3+}, Cr^{3+}, Mg^{2+}, and Co^{3+} had shown the improved selectivity of nitrogen from water [22-27].

Various deposition techniques have been applied to get Co-doped TiO_2 thin films such as sol-gel [12], chemical vapor deposition [28], pulsed laser deposition [29]. Of all the variety of deposition techniques, the sol-gel is the simplest and cheapest deposition technique [30].

This study aims to prepare titanium dioxide thin films doped with Co through the sol-gel method. The deposition process was repeated 3 times to prepare 1 to 3 layers. The structural, morphological, and optical properties of Co-doped TiO_2 thin films are evaluated.

2. Materials and Methods

To prepare Co-doped TiO_2 thin films, two solutions were prepared. The first one is 2 g of cobalt (II) acetate tetrahydrate was completely dissolved in deionized water (5cc). Afterward, the solution of ethanol and acetic acid was added to the beaker and stirred for 30 min. The second one, tetra-n-butyl orthotitanate, and ethanol were mixed with constant stirring for 15 min. After the two solutions' preparation, the second solution was added dropwise to that of the first one and kept stirring for an extra 30 min to obtain a clear homogeneous titanium dioxide doped with Co solution [12,30].

The glass substrates (2cm × 2cm) were respectively cleaned with ethanol, acetone, and deionized water in an ultrasonic cleaner in 15 min, then dried in the air. Titanium dioxide doped with Co films were coated on soda-lime glass through a homemade spin-coater with a speed of 4821 rpm for 30 sec. After each coating, layers were dried into an incubator (100 °C) for 15 min. The deposition process was done 3 times to prepare 1 to 3 layers.

To investigate titanium dioxide's structural and morphological characteristics, doped with Co thin films, an x-ray diffractometer (XRD) and scanning electron microscope (Model: DSM-960A) were utilized. XRD pattern of varying layers of titanium dioxide doped with Co films was recorded through an x-ray diffractometer (Model: STOE STADI MP) with CuK_α source (1.54 Å) in 2θ angular ranges between 10° - 90°. Furthermore, the energy-dispersive spectra analysis attached to SEM device provided the elemental and chemical content of the

samples. The optical property of films was studied by a UV-VIS spectrophotometer (Model: Varian Cary500 Scan).

3. Results and Discussion

3.1. Structural properties.

Figure 1 presents the XRD pattern of 1-3 layers of Co-doped TiO_2 films. All the films displayed amorphous nature that could be due to the low growth process at a lower temperature (100 °C in this study), as has also been reported by other research groups [31,32]. It is evident that single-layered Co-doped TiO_2 film depicted short-range crystallinity, as reported previously [33,34]; however, with increasing the thickness, the film lost the slight crystalline nature displaying higher amorphous nature suggesting the effect of film thickness on the crystallinity [33]. The same behavior was observed with Renugadevi *et al.* [34]. They found that the XRD peaks of Co-doped TiO_2 synthesized using sol-gel method peaks are not sharp, reflecting the small crystallite size. It can also be observed that the XRD pattern did not demonstrate any discrete cobalt phase indicating the uniform dispersion of cobalt ions [35].

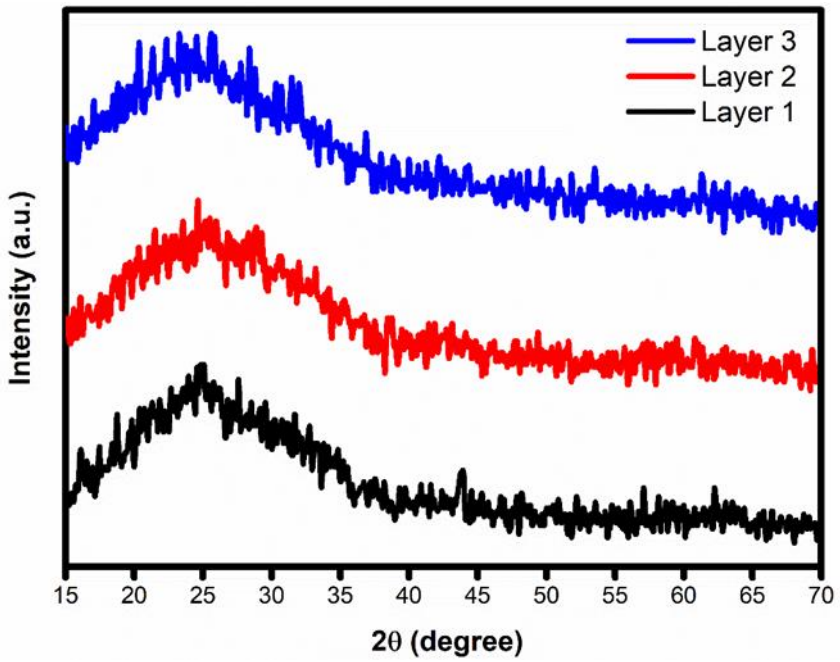

Figure 1. XRD patterns of TiO_2 doped with Co for 1- to 3- layers.

3.2. Morphological characteristics.

Figure 2 presents FESEM images of 1-3 layered Co-doped TiO_2 as-deposited films. The three micrographs depicted highly uniform TiO_2 particle alignment on the coated surface, as indicated in [36]. All the layers showcased granular TiO_2 morphology; however, the porosity was observed to decrease with the increasing film thickness with successive layering [32]. The increment of thickness leads nanoparticles to get closer, indicating the decrease of average nanoparticle size. In fact, the doping of cobalt impedes the development of the particles. [12,37,38] The surface morphology of films is identical, although the thickness is different, signifying their non-crystalline structures [39]. In addition, the lack of clusters confirms the amorphous structures of all samples that were consistent with the XRD data results (Figure 1). A significant feature of the surface of the 3-layered film was observed compared to the 1- and

2-layered Co-doped TiO_2 films; the 3-layered film showed a better adhesion and a crack-free morphology.

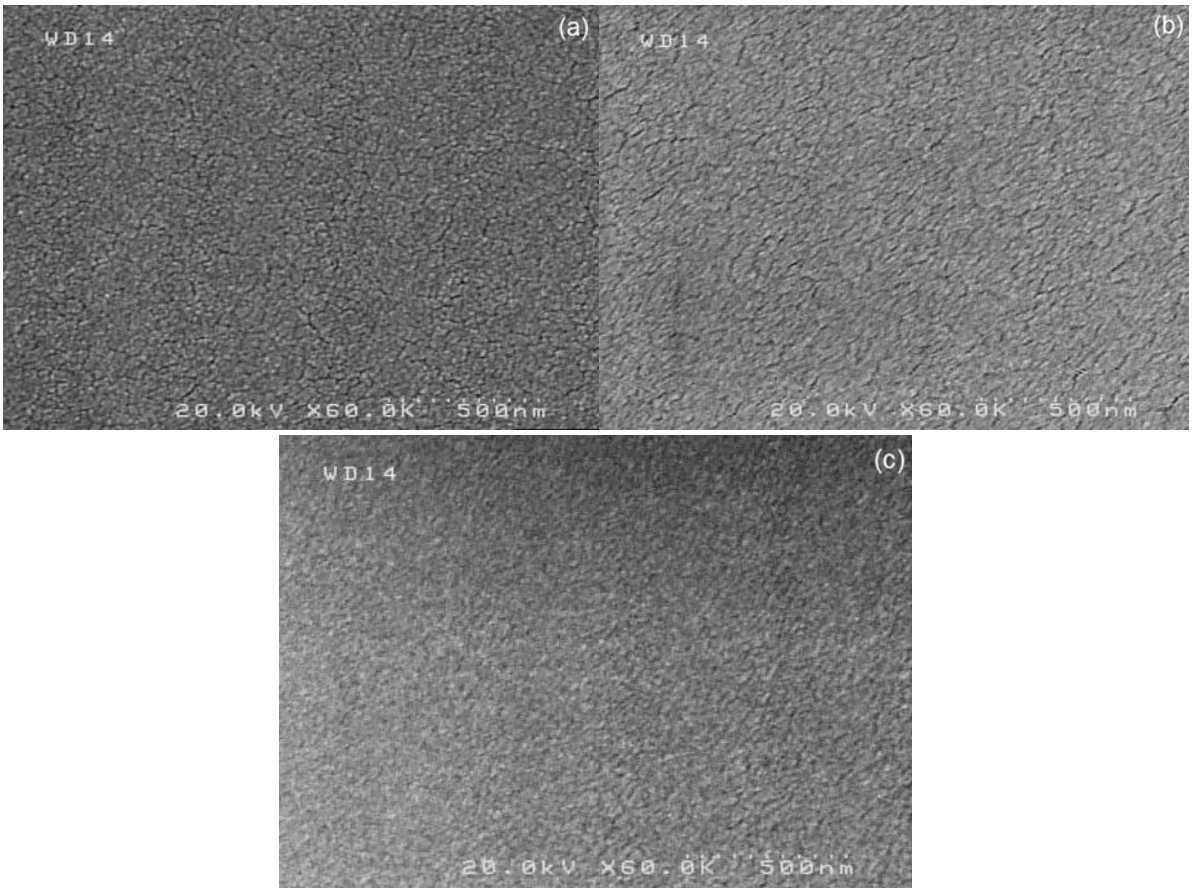

Figure 2. FESEM images of (a) 1-, (b) 2- (c) 3-layered TiO_2 thin films doped with Co.

3.3. Elemental properties.

Figure 3 indicates the EDS spectra of 1- to 3- layered Co-doped TiO_2 thin films to identify the elemental composition. The spectra verify the existence of titanium, oxygen, and cobalt. The peaks at 0.7 KeV and 6.9 KeV belong to the presence of cobalt. The good interaction of Co with TiO_2 through the sol-gel preparation method is confirmed by the less intense peak of cobalt [12,38-42].

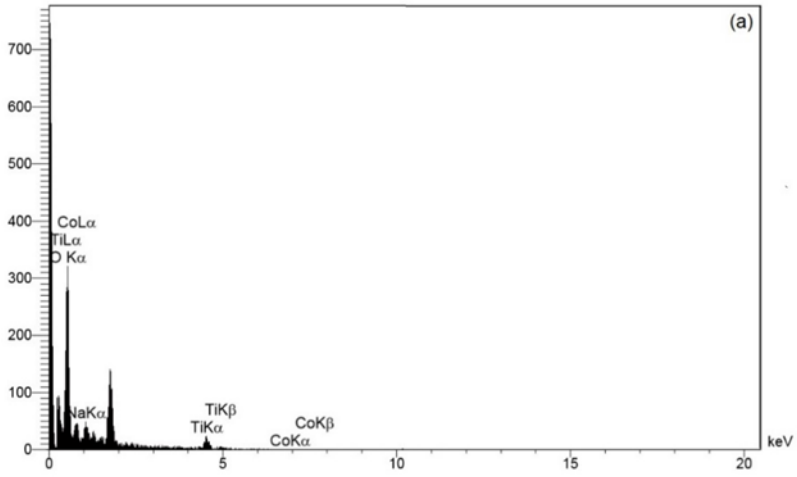

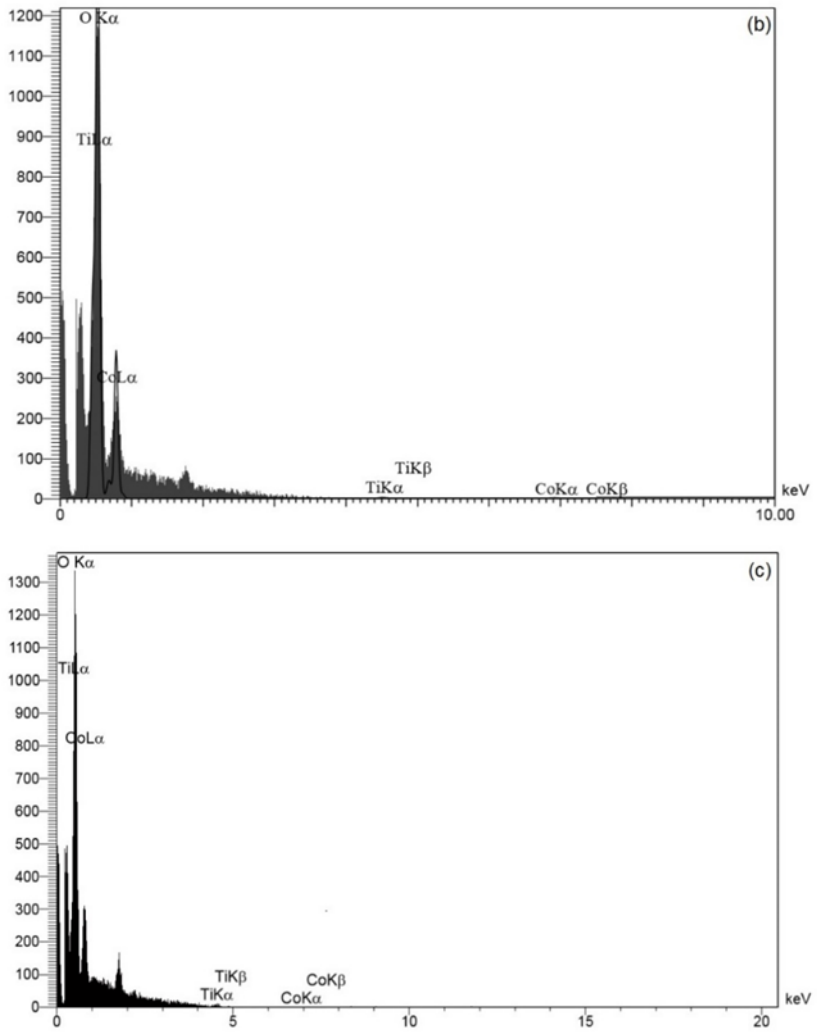

Figure 3. EDS spectra of (**a**) 1-; (**b**) 2-; (**c**) 3-layered TiO_2 doped with Co thin films.

3.4. Optical properties.

We have studied titanium dioxide doped with Co films by UV-Vis spectrophotometer. From Figure 4, TiO_2 thin films doped with Co are transparent in the visible area. This transmission spectrum confirms the preparation of Co-doped TiO_2 thin films by the sol-gel method [23,43].

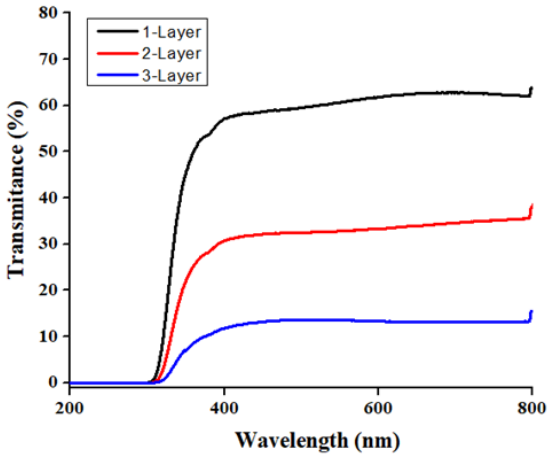

Figure 4. Transmittance spectra of multilayers of Co-TiO_2 thin films.

The as-deposited all layers Co-doped TiO_2 thin films show ~80% transmittance that reduces to ~10%, caused by the thickness difference of each layer. As the number of coating layers increased, the absorbance of the photons increased [44]. It can be attributed to the thickness change and the decrease of the average size of nanoparticles shown in FESEM images (Figure 2).

The reflectance spectra (Figure 5) are almost identical in the reflectivity minimum's peak position at 347 nm. The reflectance spectrum of 3-layered Co-coated TiO_2 film was observed to depict a contrasting pattern to the similar 1- and 2- layered coated films. The pattern's deflection could be due to the variation in the film thickness in the 3- layered coating compared to the 1- and 2- layered counterparts. The 3-layered deposited film has a low percentage of reflectance caused by an amorphous phase that can be confirmed by XRD analysis resulting in the decreased film density. In this case, these films' surface morphology has highly dense into porous and oxygen vacancy defects. The oxygen vacancy (OV) formation energy (EF*) is 5.48 eV for Co dopant, which leads to strong bonds with oxygen atoms [45]. On the other side, the defects of oxygen also reduce the reflectance that was confirmed by EDS spectra with a more intense oxygen peak and published literature [46], which indicates the dominant composition of the TiO_x films. The Co-doping content influenced to decrease the light scattering can pass through these films.

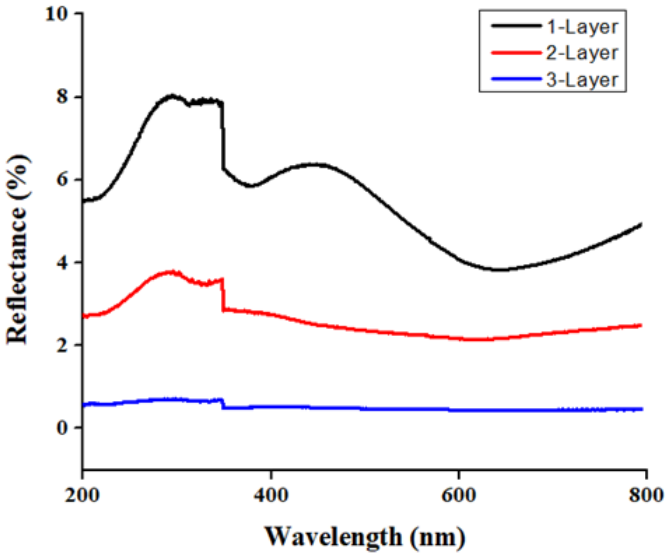

Figure 5. Reflectance spectra of Co-TiO_2 thin films.

Figure 6 shows the absorption spectrum of TiO_2 thin films doped with Co with different growth layers at room temperature. The samples' absorption spectra demonstrate the dominant absorption peak in the UV region and less in the visible region. The transfer of charge from the valence band (O_2p state) to the conduction band (Ti_3d state) was indicated by absorption bands at 200–400 nm [38]. Based on the literature [47], it was a similarity in the Te^{+4} and Co^{+2} ionic radii (68 and 72 pm) that enables the occurrence of the interstitial incorporation of cobalt ions into titanium dioxide anatase structure, and Co cation has been inserted into titanium dioxide structure and results in bandgap energy reduction [12].

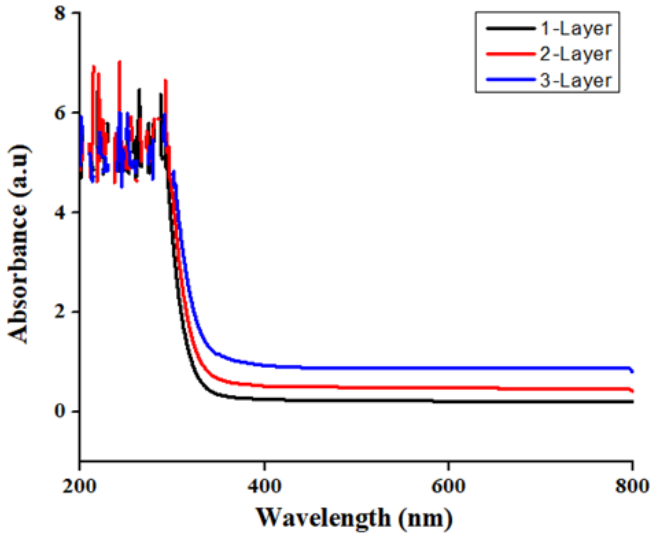

Figure 6. Absorbance spectra of Co-TiO_2 thin films.

The relationship between the photon of energy excitation versus the bandgap energy (E_g) is given by the Tauc formula [48]:

$$(\alpha h\nu)^n = A\,(h\nu - E_g) \quad (1)$$

Where A is constant, the power of n for the indirect energy gap is equal to 1/2, and for the direct energy, the gap is 2. The optical band gap energy E_g for TiO_2 thin films doped with Co is obtained by extrapolating the curve hν versus $(\alpha h\nu)^{1/2}$.

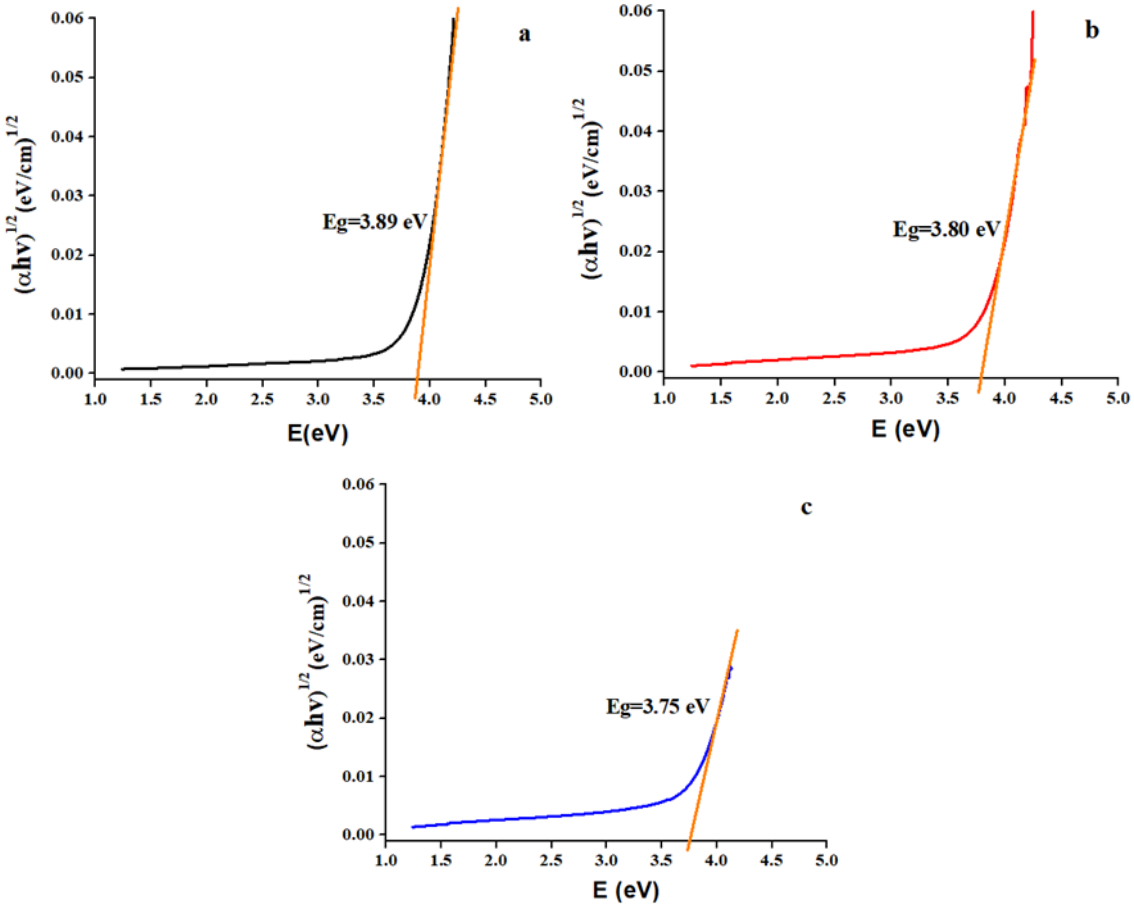

Figure 7. Indirect bandgap energy (Tauc's plot) of (a) 1-, (b) 2-, (c) 3-layered TiO_2 thin films doped with Co.

Regarding the literature [49], it was supposed that films own an indirect bandgap. Thus, the plots of $(\alpha h\nu)^{1/2}$ vs. photon energy (E) are illustrated in Figure 7.

The obtained E_g of Co-TiO_2 thin films is 3.89, 3.80, and 3.75 eV, with a thickness of 395.44, 542.70, and 793.23 nm, respectively, which are larger than the bandgap of bulk TiO_2 ~3.20 eV [50], as well as the values published in the literature (3.44–3.64 eV) [51,52]. As expected, the value of the indirect bandgap decreased with the thickness of layers increased. This can be due to the increment of defects in the forbidden band. The bandgap energy decreased from 3.89 eV for 1-layered Co-doped TiO_2 thin film to 3.80 eV for 2-layered and further decrement to 3.75 eV for 3-layered. The variation of the indirect bandgap is a minute decrease of about 0.14 eV. Further, there are no reports of the higher bandgap energy of Co-doped TiO_2 as-deposited films grown by sol-gel method without annealing.

Furthermore, the extended states of the width below the conduction band are represented with Urbach energy given by equation [53]:

$$\alpha=\alpha_0 \exp(\frac{E}{E_U}) \quad (2)$$

where α is the coefficient of absorption, α_0 is constant, E is the photon's energy, and E_U is the Urbach energy.

The experimental value proposed with the Urbach energy empirical relationship between the straight line slope of Lnα vs. photon energy plot (Figure 8), using the following equation:

$$Ln(\alpha)=Ln(\alpha_0)-(\frac{h\nu}{E_U}) \quad (3)$$

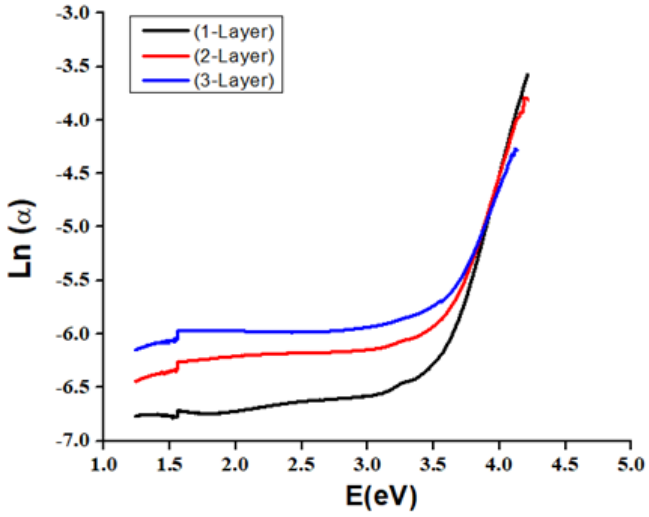

Figure 8. Urbach energy of 1-layered, 2-layered, 3-layered TiO_2 thin films doped with Co.

The refractive index is an optical property that is essential for materials to be applied in optical devices. We proposed to determine the refractive index by the following Herve and Vandamme relation [54]:

$$n^2 = 1 + (\frac{A}{E_g + B})^2 \quad (4)$$

where A = 13.6, B = 3.4, E_g is bandgap energy, and n is the refractive index of the film.

The values of bandgap energy (E_g), Urbach energy, and refractive index for TiO_2 thin films doped with Co are tabulated in Table 1. It is found that the Eg values decreased with

increasing doping thickness, indicating a positive effect of Co^{2+} on the activation under UV-Visible. Douven *et al*. [55] found a similar positive effect when using iron and nitrogen-doped with TiO_2. Consequently, Urbach energy increased from 0.215 to 0.275 eV, as Ghasemi et al. [56] reported that Urbach energy increased from 237.64 to 257.2 meV. This shift indicates that there have been band-to-tail and tail-to-tail transitions [57], which is because of an increase in the oxygen defect in the host structure of TiO_2 [58]. This may be attributed to the high density of defects throughout the intergranular regions, leading to the optical energy gap reduction. Urbach energy increases with increasing refractive index and the film thickness. The refractive index varies from 2.12 to 2.15 with increasing thickness. The value of the refractive index of the 3-layered film was the same as reported by Ref [59], Co-doped TiO_2 film annealed at 400°C. Other researchers have reported refractive index values between 2.35–2.40 with increasing cobalt concentrations, indicating that the crystallinity of film becomes dense [60].

Table 1. Comparison of values of bandgap, Urbach energy, and refractive index of Co-doped TiO_2 as-deposited films.

Co-doped TiO_2	Tickness (nm)	Bandgap (eV)	Urbach energy (eV)	Refractive index
1-layer	395.44	3.89	0.215	2.12
2-layer	542.70	3.80	0.246	2.14
3-layer	793.23	3.75	0.275	2.15

Table 1 indicates that the thickness of 1-layered (E_g=3.89 eV), 2-layered (E_g=3.80 eV), and 3-layered (E_g=3.75 eV) film are found to be 395.44, 542.70, and 793.23 nm, respectively. The 3-layered film thickness shows a significant effect on the absorption band. The thicker film has a relative reduction in the absorption and bandgap energy confirmed by the XRD spectra, as shown in Figure 1. The 3-layered film is amorphous, as shown by the lower percentage of reflectance. It can possibly happen as the Co dopant is embedded in the TiO_2 matrix. The increase in Co dopant can cause greater crystallization into large particles due to greater deposition time as-deposited films by a spin-coater. It can be interpreted that the bandgap energy decreases with the increase of thickness because the film crystallinity also increases in the crystallite size. Interestingly, our results for the 3-layered film are similar to the calculated bandgap energy of 3.75 eV (330 nm) for annealed Co-doped TiO_2 nanoparticle at 500°C with 8 wt% of Co^{2+} via sol-gel method [38].

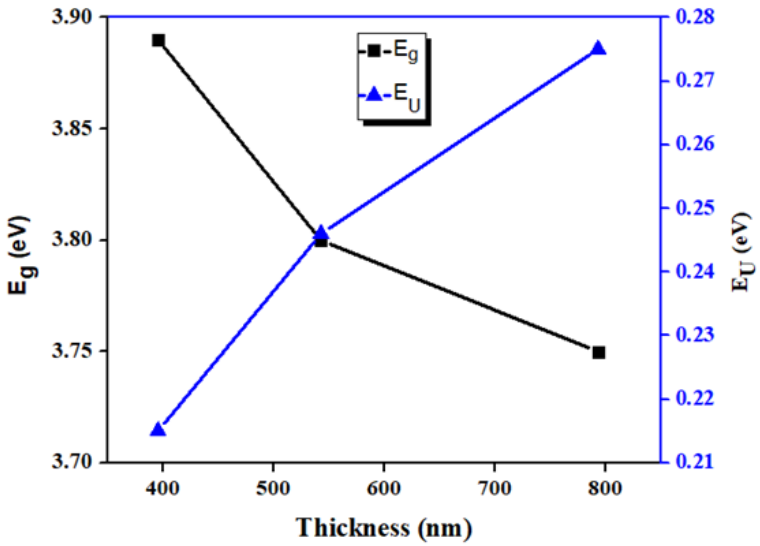

Figure 9. Comparison of optical band gap and Urbach energy of Co-TiO_2 thin films with different thicknesses of 395.44 nm, 542.70 nm, and 793.23 nm.

Figure 9 shows the dependence between bandgap energy and the Urbach energy for the film with thicknesses of 395.44 nm, 542.70 nm, and 793.23 nm. Note that with the increase of thickness, the bandgap's value increases, and Urbach energy decreases. Urbach energy increases from 0.215 to 0.275 eV as the bandgap energy decreases because of the donor's level into impurity bands. These Urbach energy values are close to those reported by Ref. [59], in which the Urbach energy of Co-doped TiO_2 films observed from 0.237 to 0.257 eV with the addition of Co. Co-dopant content causes band-tailings due to the level of donor broadening into the impurities band merging with the conduction band [61]. It is similar to decrease the bandgap energy with increasing Urbach energy in the nanocrystals of TiO_2 doped with Cr prepared by a sol-gel method [62].

4. Conclusions

Titanium dioxide thin films doped with Co were fabricated through the sol-gel method. EDS spectra verified the existence of elements used in the samples. XRD patterns displayed the amorphous nature of films due to the low growth process at lower temperatures. FESEM images showed a highly uniform particles alignment on the surface. The transparency of thin films was reduced with increasing the thickness that is attributed to the decrease of the average size of nanoparticles. The absorption spectra demonstrate a dominant absorption peak in the UV region. The absorption bands at 200–400 nm indicate a transfer of charge from the valence band (O_{2p} state) to the conduction band. It also could be observed that with increment thickness, bandgap energy decreases, and, consequently, the Urbach energy increased.

Funding

This research received no external funding.

Acknowledgments

This experiment was conducted in Science and Research Branch, I. Azad University, Tehran, Iran.

Conflicts of Interest

The authors declare no conflict of interest.

References

1. Riaz, S.; Park, S.-Jin. An overview of TiO_2-based photocatalytic membrane reactors for water and wastewater treatments. *J. Ind. Eng. Chem.* **2020**, *84*, 23-41. https://doi.org/10.1016/j.jiec.2019.12.021.
2. Hoseinzadeh, T.; Solaymani, S.; Kulesza, S.; Achour, A.; Ghorannevis, Z.; Ţălu, Ş.; Bramowicz, M.; Ghoranneviss, M.; Rezaee, S.; Boochani, A.; Mozaffari. N. Microstructure, fractal geometry and dye-sensitized solar cells performance of CdS/TiO_2 nanostructures. *J. Electroanal. Chem.* **2018,** *830–831*, 80-87. https://doi.org/10.1016/j.jelechem.2018.10.037.
3. Chibani, O.; Challali, F.; Touam, T.; Chelouche, A.; Djouadi, D. Optical waveguiding characteristics of TiO_2 sol–gel thin films for photonic devices: effects of thermal annealing. *Opt. Eng.* **2019,** *58*, 047101. https://doi.org/10.1117/1.OE.58.4.047101.
4. Zuccaro, C.; Ghosh, I.; Urban, K.; Klein, N.; Penn, S.; Alford, N.M. Materials for HTS-shielded dielectric resonators. *IEEE Trans. Appl. Supercond.* **1997,** *7*, 3715–3718. https://doi.org/10.1109/77.622225.

5. Ning, X.-b.; Wang, X.-t.; Shao, Q.; Ge, S.-s.; Chi, L.-f. You-bo Nan, Hao Liang, Bao-rong Hou, ZnPc/TiO_2 composites for photocathodic protection of 304 stainless steel. *J. Electroanal. Chem.* **2020,** *585*, 113802. https://doi.org/10.1016/j.jelechem.2019.113802.
6. Qian, Y.; Du, J.; Kang, D.J. Enhanced electrochemical performance of porous Co-doped TiO_2 nanomaterials prepared by a solvothermal method. *Microporous Mesoporous Mater* **2019,** *273*, 148–155. https://doi.org/10.1016/j.micromeso.2018.06.056.
7. Fujisawa, J.-i. Interfacial charge-transfer transitions between TiO_2 and indole. *Chem. Phys. Lett.* **2020,** *739*, 136974. https://doi.org/10.1016/j.cplett.2019.136974.
8. Wu, Z.; Yuan, D.; Lin, S.; Guo, W.; Zhan, D.; Sun, L.; Lin, C. Enhanced photoelectrocatalytic activity of Bi_2S_3–TiO_2 nanotube arrays hetero-structure under visible light irradiation. *Int. J. Hydrog. Energy* **2020,** *45*, 32012-32021. https://doi.org/10.1016/j.ijhydene.2020.08.258.
9. Yu, J.; Zou, J.; Xu, P.; He, Q. Three-dimensional photoelectrocatalytic degradation of the opaque dye acid fuchsin by Pr and Co co-doped TiO_2 particle electrodes. *J. Clean. Prod.* **2020,** *251*, 119744. https://doi.org/10.1016/j.jclepro.2019.119744.
10. Bao, X.; Li, H.; Wang, Z.; Tong, F.; Liu, M.; Zheng, Z.; Wang, P.; Cheng, H.; Liu, Y.; Dai, Y.; Fan, Y.; Li, Z.; Huang, B. TiO_2/Ti_3C_2 as an efficient photocatalyst for selective oxidation of benzyl alcohol to benzaldehyde. *Appl. Catal. B- Environ.* **2021,** *286*, 119885. https://doi.org/10.1016/j.apcatb.2021.119885.
11. Sadanandam, G.; Luo, X.; Chen, X.; Bao, Y.; Homewood, K.P.; Gao, Y. Cu oxide quantum dots loaded TiO_2 nanosheet photocatalyst for highly efficient and robust hydrogen generation. *Appl. Surf. Sci.* **2021,** *541*, 148687. https://doi.org/10.1016/j.apsusc.2020.148687.
12. Mozaffari, N.; Elahi, S.M.; Parhizgar, S.S. Deposition of TiO_2 Multilayer Thin Films Doped with Cobalt and Studying the Effect of Annealing Temperatures and Number of Layers on the Structural and Morphological of Thin Films. *Int. J. Thermophys.* **2019.** *40*, 67. https://doi.org/10.1007/s10765-019-2533-1.
13. Mohapatra, J.; Xing, M.; Elkins, J.; Ping Liu, J. Hard and semi-hard magnetic materials based on cobalt and cobalt alloys. *J. Alloys Compd.* **2020,** *824*, 153874. https://doi.org/10.1016/j.jallcom.2020.153874.
14. Madkhli, A.Y.; Shirbeeny, W. The effect of cobalt ions doping on the optical properties of ZnS quantum dots according to photoluminescence intensity and crystalline structure. *Physica B Condens. Matter* **2020,** *597*, 412414. https://doi.org/10.1016/j.physb.2020.412414.
15. Pubby, K.; Babu, K.V.; Narang, S.B.; Magnetic, elastic, dielectric, microwave absorption and optical characterization of cobalt-substituted nickel spinel ferrites. *Mater. Sci. Eng., B* **2020,** *225*, 114513. https://doi.org/10.1016/j.mseb.2020.114513.
16. Liu, C.; Wang, F.; Zhu, S.; Xu, Y.; Liang, Q.; Chen, Z. Controlled charge-dynamics in cobalt-doped TiO_2 nanowire photoanodes for enhanced photoelectrochemical water splitting. *Colloid Interface Sci.* **2018,** *513*, 403–411. https://doi.org/10.1016/j.jcis.2018.07.003.
17. Suriyachai, N.; Chuangchote, S.; Laosiripojana, N.; Champreda, V.; Sagawa, T. Synergistic Effects of Co-Doping on Photocatalytic Activity of Titanium Dioxide on Glucose Conversion to Value-Added Chemicals. *ACS Omega* **2020,** *5*, 20373. 10.1021/acsomega.0c02334.
18. Soares, G.B.; Ribeiro, R.A.P.; de Lazaro, S.R.; Ribeiro, C. Photoelectrochemical and theoretical investigation of the photocatalytic activity of TiO_2 : N. *RSC Adv.* **2016,** *6*, 89687–89698. https://doi.org/10.1039/C6RA15825K.
19. He, X.; Yang, C.P.; Zhang, G.L.; Shi, D.W.; Huang, Q.A.; Xiao, H.B.; Liu, Y.; Xiong, R. Supercapacitor of TiO_2 nanofibers by electrospinning and KOH treatment. *Mater. Des.* **2016,** *106*, 74–80. https://doi.org/10.1016/j.matdes.2016.05.025.
20. Chanda, A.; Rout, K.; Vasundhara, M.; Joshi, S.R.; Singh, J. Structural and magnetic study of undoped and cobalt doped TiO_2 nanoparticles. *RSC Adv.* **2018,** *8*, 10939–10947. https://doi.org/10.1039/C8RA00626A.
21. Dubey, R.S.; Singh, S. Investigation of structural and optical properties of pure and chromium doped TiO_2 nanoparticles prepared by solvothermal method. *Results Phys.* **2017,** *7*, 1283-1288. https://doi.org/10.1016/j.rinp.2017.03.014.
22. Kominami, H.; Nakaseko, T.; Shimada, Y.; Furusho, A.; Inoue, H.; Murakami, S.; Kera, Y.; Ohtani, B. Selective photocatalytic reduction of nitrate to nitrogen molecules in an aqueous suspension of metal-loaded titanium(iv) oxide particles. *ChemComm.* **2005,** 2933-2935. https://doi.org/10.1039/B502909K.
23. Kominami, H.; Furusho, A.; Murakami, S.; Inoue, H.; Kera, Y.; Ohtani, B. Effective Photocatalytic Reduction of Nitrate to Ammonia in an Aqueous Suspension of Metal-Loaded Titanium (IV) Oxide Particles in the Presence of Oxalic Acid. *Catal. Lett.* **2001,** *76*, 31–34. https://doi.org/10.1023/A:1016771908609.

24. Kudo, A.; Domen, K.; Maruya, K.-I.; Onishi, T. Reduction of nitrate ions into nitrite and ammonia over some photocatalysts. *J. Catal.* **1992,** *135*, 300. https://doi.org/10.1016/0021-9517(92)90287-R.
25. Ranjit, K.T.; Varadarajan, T.K.; Viswanathan, B. Photocatalytic reduction of nitrite and nitrate ions to ammonia on Ru/TiO_2 catalysts. *J. Photochem. Photobiol. A* **1995,** *89*, 67 -68. https://doi.org/10.1016/1010-6030(94)04029-2.
26. Ranjit, K.T.; Viswanathan, B. Photocatalytic reduction of nitrite and nitrate ions to ammonia on M/TiO_2 catalysts. *J. Photochem. Photobiol. A* **1997,** *107*, 215. https://doi.org/10.1016/S1010-6030(96)04505-4.
27. Zhu, H.; Chen, X.; Zheng, Z.; Ke, X.; Jaatinen, E.; Zhao, J.; Guo, C.; Xie, T.; Wang, D. Mechanism of supported gold nanoparticles as photocatalysts under ultraviolet and visible light irradiation. *ChemComm.* **2009,** *48*, 7524-7526. https://doi.org/10.1039/B917052A.
28. Méndez-Lozano, N.; Apátiga-Castro, M.; Manzano-Ramírez, A.; Rivera-Muñoz, E. M.; Velázquez-Castillo, R.; Alberto-González, C.; Zamora-Antuñano, M. Morphological study of TiO_2 thin films doped with cobalt by Metal Organic Chemical Vapor Deposition. *Results Phys.* **2020,** *16*, 102891. https://doi.org/10.1016/j.rinp.2019.102891.
29. Gong, B.; Luo, X.; Bao, N.; Ding, J.; Li, S.; Yi, J. XPS study of cobalt doped TiO_2 films prepared by pulsed laser deposition. *Surf. Interface Anal.* **2014,** *46*, 1043–1046. https://doi.org/10.1002/sia.5397.
30. Mozaffari, N.; Elahi, S.H.; Parhizgar, S.S.; Mozaffari, N.; Elahi, S.M. The effect of annealing and layer numbers on the optical and electrical properties of cobalt-doped TiO_2 thin films. *Mater. Res. Express* **2019,** *6*, 116428. https://doi.org/10.1088/2053-1591/ab4662.
31. Zhu, W.; Xu, Y.; Li, H.; Dai, B.; Xu, H.; Wang, C.; Chao, Y.; Liu, H. Photocatalytic oxidative desulfurization of dibenzothiophene catalyzed by amorphous TiO_2 in ionic liquid. *Korean J. Chem. Eng.* **2014,** *31*, 211–217. https://doi.org/10.1007/s11814-013-0224-3.
32. Grilli, M.L.; Yilmaz, M.; Aydogan, S.; Cirak, B.B. Room temperature deposition of XRD-amorphous TiO_2 thin films: Investigation of device performance as a function of temperature. *Ceram. Int.* **2018,** *44*, 11582–11590. https://doi.org/10.1016/j.ceramint.2018.03.222.
33. Nair, P.B.; Justinvictor, V.B.; Daniel, G.P.; Joy, K.; Thomas, P.V. Influence of film thickness and annealing atmosphere on the structural, optical and luminescence properties of nanocrystalline TiO_2 thin films prepared by RF magnetron sputtering. *J. Mater. Sci.: Mater. Electron.* **2013,** *24*, 2453–2460. https://doi.org/10.1007/s10854-013-1117-2.
34. Renugadevi, R.; Venkatachalam, T.; Narayanasamy, R.; Dinesh Kirupha, S. Preparation of Co doped TiO_2 nano thin films by Sol Gel technique and photocatalytic studies of prepared films in tannery effluent. *Optik* **2016,** *127*, 10127–10134. https://doi.org/10.1016/j.ijleo.2016.07.090.
35. Sadanandam, G.; Lalitha, K.; Kumari, V.D.; Shankarb, M.V.; Subrahmanyam, M. Cobalt doped TiO_2: A stable and efficient photocatalyst for continuous hydrogen production from glycerol: Water mixtures under solar light irradiation. *Int. J. Hydrog. Energy* **2013,** *38*, 9655-9664. https://doi.org/10.1016/j.ijhydene.2013.05.116.
36. Momenin, M.M.; Ghayeb, Y. Preparation of cobalt coated TiO_2 and WO_3–TiO_2 nanotube films via photo-assisted deposition with enhanced photocatalytic activity under visible light illumination. *Ceram. Int.* **2016,** *42*, 7014-7022. https://doi.org/10.1016/j.ceramint.2016.01.089.
37. Xu, J.; Shi, S.; Li, L.; Zhang, X.; Wang, Y.; Chen, X.; Wang, J.; Lv, L.; Zhang, F.; Zhong, W. Structural, optical, and ferromagnetic properties of Co-doped TiO_2 films annealed in vacuum. *J. Appl. Phys.* **2010,** *107*, 053910. https://doi.org/10.1063/1.3319556.
38. Mugundan, S.; Rajamannan, B.; Viruthagiri, G.; Shanmugam, N.; Gobi, R.; Praveen, P. Synthesis and characterization of undoped and cobalt-doped TiO_2 nanoparticles via sol–gel technique. *Appl. Nanosci.* **2015,** *5*, 449–456. https://doi.org/10.1007/s13204-014-0337-y.
39. Ebrahimian, A.; Monazzam, P.; Fakhari Kisomi, B. Co/TiO_2 nanoparticles: preparation, characterization and its application for photocatalytic degradation of methylene blue. *Desalin. water treat.* **2017,** *63*, 283–292. 10.5004/dwt.2017.20205.
40. Venkatachalam, N.; Palanichamy, M.; Arabindoo, B.; Murugesan, V. Enhanced photocatalytic degradation of 4-chlorophenol by Zr^{4+} doped nano TiO_2. *J. Mol. Catal. A Chem.* **2007,** *266*, 158–165. https://doi.org/10.1016/j.molcata.2006.10.051.
41. Hamadanian, M.; Reisi-Vanani, A.; Majedi, A. Sol-gel preparation and characterization of Co/TiO_2 nanoparticles: Application to the degradation of methyl orange. *J. Iran. Chem. Soc.* **2010,** *7*, 52–58. https://doi.org/10.1007/BF03246184.

42. Ju, Y.; Wang, M.; Wang, Y.; Wang, S.; Fu, C. Electrical Properties of Amorphous Titanium Oxide Thin Films for Bolometric Application. *Adv. Condens. Matter Phys.* **2013,** *2013*, 5. https://doi.org/10.1155/2013/365475.
43. Boutlala, A.; Bourfaa, F.; Mahtili, M.; Bouaballou, A. Deposition of Co-doped TiO_2 Thin Films by sol-gel method. *IOP Conf. Ser.: Mater. Sci. Eng.* **2016,** *108*, 012048. https://doi.org/10.1088/1757-899X/108/1/012048.
44. Chanda, A.; Ram Joshi, S.; Akshay, V. R.; Varma, S.; Singh, J.; Vasundhara, M.; Shukla, P. Structural and optical properties of multilayered un-doped and cobalt doped TiO_2 thin films. *Appl. Surf. Sci.* **2021,** *536*, 147830. https://doi.org/10.1016/j.apsusc.2020.147830.
45. González-Torres, J.C.; Cipriano, L.A.; Poulain, E.; Domínguez-Soria, V.; García-Cruz, R.; Olvera-Neria, O. Optical properties of anatase TiO_2: synergy between transition metal doping and oxygen vacancies. *J. Mol. Model.* **2018,** *24*, 1-11. https://doi.org/10.1007/s00894-018-3816-3.
46. Banakh, O.; Schmid, P.E.; Sanjines, R.; Levy, F. Electrical and optical properties of TiO_x thin films deposited by reactive magnetron sputtering. *Surf. Coat. Technol.* **2002,** *151–152*, 272–275. https://doi.org/10.1016/S0257-8972(01)01605-X.
47. Ghasemi, S.; Rahimnejad, S.; Rahman, S.S.; Rohani, S.; Gholami, M.R. Transition metal ions effect on the properties and photocatalytic activity of nanocrystalline TiO_2 prepared in an ionic liquid. *J. Hazard. Mater.* **2009,** *172*, 1573–1578. https://doi.org/10.1016/j.jhazmat.2009.08.029.
48. El-Gammal, O.A.; Alsayed Fouda, A. E.; Mohamed Nabih, D. Synthesis, spectral characterization, DFT and in vitro antibacterial activity of Zn(II), Cd(II) and Hg(II) complexes derived from a new thiosemicarbazid. *Lett. Appl. NanoBioScience* **2019,** *8*, 715 – 722. https://doi.org/10.33263/LIANBS84.715722.
49. Mostaghni, F.; Abed, Y. Structural determination of Co/TiO_2 nanocomposite: XRD technique and simulation analysis. *Mater. Sci.-Poland* **2016,** *34*, 534-539. https://doi.org/10.1515/msp-2016-0071.
50. Tang, H.; Berger, H.; Schmid, P.E.; Lévy, F.; Burri, G. Photoluminescence in TiO_2 anatase single crystals. *Solid State Commun.* **1993,** *87*, 847–850. https://doi.org/10.1016/0038-1098(93)90427-O.
51. Hu, Z.G.; Li, W.W. ; Wu, J.D. ; Sun, J.; Shu, Q.W. ; Zhong, X.X.; Zhu, Z.Q.; Chu, J.H. Optical properties of pulsed laser deposited rutile titanium dioxide films on quartz substrates determined by Raman scattering and transmittance spectra. *Appl. Phys. Lett.* **2008,** *93*, 181910. https://doi.org/10.1063/1.3021074.
52. Mahmoud A.E.D. Nanomaterials: Green Synthesis for Water Applications. In: Kharissova O., Martínez L., Kharisov B. (eds) Handbook of Nanomaterials and Nanocomposites for Energy and Environmental Applications. Springer, Cham. **2020**; 1-21. https://doi.org/10.1007/978-3-030-11155-7_67-1.
53. Abushad, M.; Arshad, M.; Naseem, S.; Husain, S.; Khan, W. Role of Cr doping in tuning the optical and dielectric properties of TiO_2 nanostructures. *Mater. Chem. Phys.* **2020,** *256*, 123641. https://doi.org/10.1016/j.matchemphys.2020.123641.
54. Herve, P.J.L.; Vandamme, L.K.J. General relation between refractive index and energy gap in semiconductors. *Infrared Phys. Technol.* **1994,** *35*, 609-615. https://doi.org/10.1016/1350-4495(94)90026-4.
55. Douven, S.; Mahy, J.G.; Wolfs, C.; Reyserhove, C.; Poelman, D.; Devred, F.; Gaigneaux, E. M. ; Lambert, S.D. Efficient N, Fe Co-Doped TiO_2 Active under Cost-Effective Visible LED Light: From Powders to Films. *Catalyst* **2020,** *10*, 547. https://doi.org/10.3390/catal10050547.
56. Bhat, S.; Sandeep, K.M.; Kumar, P.; Dharmaprakash, S.M.; Byrappa, K. Characterization of transparent semiconducting cobalt doped titanium dioxide thin films prepared by sol–gel process. *J. Mater. Sci.: Mater. Electron.* **2018,** *29*, 1098–1106. https://doi.org/10.1007/s10854-017-8011-2.
57. Ferreira, V.C.; Nunes, M.R.; Silvestre, A.J.; Monteiro, O.C. Synthesis and properties of Co-doped titanate nanotubes and their optical sensitization with methylene blue. *Mater. Chem. Phys.* **2013,** *142*, 355-362. https://doi.org/10.1016/j.matchemphys.2013.07.029.
58. Subramanian, M.; Vijayalakshmi, S.; Venkataraj, S.; Jayavel, R. Effect of cobalt doping on the structural and optical properties of TiO_2 films prepared by sol–gel process. *Thin Solid Films* **2008,** *516*, 3776–3782. https://doi.org/10.1016/j.tsf.2007.06.125.
59. Khalaf, M.M.; El-Lateef, H.M.A.; Ali, H.M. Optical and Photocatalytic Measurements of Co-TiO_2 Nanoparticle Thin Films. *Plasmonics* **2018,** *13*, 1795–1802. https://doi.org/10.1007/s11468-018-0693-7.
60. Tian, J.; Deng, H.; Sun, L.; Kong, H.; Yang, P.; Chu, J. Effects of Co doping on structure and optical properties of TiO_2 thin films prepared by sol–gel method. *Thin Solid Films* **2012,** *520*, 5179–5183. https://doi.org/10.1016/j.tsf.2012.03.125.

61. Nam, G.; Yoon, H.; Kim, B.; Lee, D.-Y.; Kim, J.S.; Leem, J.-Y. Effect of Co doping concentration on structural properties and optical parameters of Co-doped ZnO thin films by sol-gel dip-coating method. *J. Nanosci. Nanotechnol.* **2014,** *14*, 8544–8548. https://doi.org/10.1166/jnn.2014.9982.
62. Akshay, V.R.; Arun, B.; Mandal, G.; Vasundhara, M. Visible range optical absorption, Urbach energy estimation and paramagnetic response in Cr-doped TiO_2 nanocrystals derived by a sol–gel method. *Phys. Chem. Chem.* **2019,** *21*, 12991-13004. https://doi.org/10.1039/C9CP01351B.